The EMBO Journal (2013) 32, 1613–1625
www.embojournal.org

TRANSPARENT PROCESS

THE EMBO JOURNAL

The transcription factor Hmx1 and growth factor receptor activities control sympathetic neurons diversification

Alessandro Furlan[1], Moritz Lübke[1], Igor Adameyko[1], Francois Lallemend[2] and Patrik Ernfors[1,3,*]

[1]Division of Molecular Neurobiology, Department of Medical Biochemistry and Biophysics, Karolinska Institutet, Stockholm, Sweden, [2]Department of Neuroscience, Karolinska Institutet, Stockholm, Sweden and [3]Stellenbosch Institute for Advanced Study (STIAS), Wallenberg Research Center at Stellenbosch University, Stellenbosch, South Africa

The sympathetic nervous system relies on distinct populations of neurons that use noradrenaline or acetylcholine as neurotransmitter. We show that fating of the sympathetic lineage at early stages results in hybrid precursors from which, genetic cell-lineage tracing reveals, all types progressively emerge by principal mechanisms of maintenance, repression and induction of phenotypes. The homeobox transcription factor HMX1 represses *Tlx3* and *Ret*, induces *TrkA* and maintains *tyrosine hydroxylase (Th)* expression in precursors, thus driving segregation of the noradrenergic sympathetic fate. Cholinergic sympathetic neurons develop through cross-regulatory interactions between TRKC and RET in precursors, which lead to *Hmx1* repression and sustained *Tlx3* expression, thereby resulting in failure of *TrkA* induction and loss of maintenance of *Th* expression. Our results provide direct evidence for a model in which diversification of noradrenergic and cholinergic sympathetic neurons is based on a principle of cross-repressive functions in which the specific cell fates are directed by an active suppression of the expression of transcription factors and receptors that direct the alternative fate.

The EMBO Journal (2013) **32,** 1613–1625. doi:10.1038/emboj.2013.85; Published online 16 April 2013
Subject Categories: development; neuroscience
Keywords: cholinergic; development; homeobox; neurotropic factors; noradrenergic

Introduction

The paravertebral sympathetic nervous system is organized as a chain of ganglia along the rostro-caudal axis of the vertebra receiving preganglionic innervation from central nervous system neurons located in the spinal cord. Most sympathetic neurons differentiate into noradrenergic neurons, which innervate internal organs regulating their function, for instance gut motility, salivation, piloerection, pupil diameter and vasoconstriction. Some sympathetic neurons instead differentiate into cholinergic neurons. Sympathetic cholinergic neurotransmission is believed to play unique roles compared to the noradrenergic, innervating the periosteum (Asmus *et al*, 2000), and is particularly important during thermoregulation by innervating sweat glands and stimulating perspiration. In mammals, apart from rodents, cholinergic sympathetic vasodilator nerves also innervate muscle vasculature (Morris *et al*, 1998; Ernsberger and Rohrer, 1999), which actively redistributes oxygen and nutrients to the working muscle (Anderson *et al*, 2006).

A sympathetic fate defined by a regulatory network of transcription factors is induced by bone morphogenetic proteins (BMPs) expressed in the dorsal aorta acting on migrating neural crest cells (NCCs; Schneider *et al*, 1999). The paired-like homeodomain transcription factor PHOX2B and the bHLH protein HAND2 are required for defining a noradrenergic sympathetic fate (Hirsch *et al*, 1998; Lo *et al*, 1998; Pattyn *et al*, 1999; Howard, 2005; Lucas *et al*, 2006). PHOX and HAND factors drive expression of the noradrenaline biosynthesis enzymes tyrosine hydroxylase (TH) and dopamine-β-hydroxylase (DBH) in sympathetic precursors. Thus, development of the sympathetic lineage is governed by an early gene-regulatory network likely defining early aspects of sympathetic neuron precursors (Apostolova and Dechant, 2009). In later development, diversification of sympathetic neurons into the distinct functional types is believed to be governed by extrinsic soluble signals (Habecker and Landis, 1994; Asmus *et al*, 2001). However, the transcriptional regulators and their mechanistic interactions with environmental signals during diversification of sympathetic neurons into the distinct types remain largely unknown.

The H6 homeobox gene *Hmx1* (*Nkx5-3*) caught our attention as a possible candidate for regulation of cell type specification in the neural crest, as initiation of its expression coincides with neurogenesis and becomes restricted to only a few neural crest-derived neurons later in development (Yoshiura *et al*, 1998; Adameyko *et al*, 2009; Munroe *et al*, 2009). A mutation in *Hmx1* causes the autosomal recessive Oculo-Auricular syndrome in humans, characterized by malformation of the eyes and external ears (Schorderet *et al*, 2008), and Dumbo mice containing a mutation in *Hmx1* substantially recapitulate the human condition (Munroe *et al*, 2009). Here, we report that induction of the sympathetic fate results in a hybrid precursor population that diversifies into distinct neuronal types by initiation of *Hmx1* expression in a mechanism involving the activity by different classes of growth factor receptors.

Results

Hierarchical development of sympathetic subtypes

While expression of noradrenergic traits in developing sympathetic precursors is well documented, direct quantitative

*Corresponding author. Division of Molecular Neurobiology, Department of Medical Biochemistry and Biophysics, Karolinska Institutet, Scheelesv 1, 17177 Stockholm, Sweden.
Tel.: +46 8524 876 59; Fax: +46 341 960; E-mail: patrik.ernfors@ki.se

Received: 15 January 2013; accepted: 15 March 2013; published online: 16 April 2013

measurements of segregation of noradrenergic and cholinergic fates in early sympathetic precursors remain to be described (Goridis and Rohrer, 2002; Howard, 2005; Apostolova and Dechant, 2009). To understand if mechanisms operating during sympathetic neuron consolidation into distinct types encompass the extinction of phenotypes already existing in precursors, we first examined noradrenergic and cholinergic associated markers in E12.5 paravertebral thoracic level 9–13 sympathetic ganglia (SG) neurons. The enzymes in noradrenalin synthesis TH, DBH, vesicular monoamine transporter (VMAT2), the enzyme for acetylcholine biosynthesis (choline acetyltransferase (ChAT)), the vesicular acetylcholine transporter (VAChT), the glial cell line-derived factor (GDNF) family ligand receptor RET, and the neurotrophin-3 (NT3) receptor, TRKC, as well as peripherin (PRPH) were abundantly present (Figure 1A). All ISL1$^+$ precursors contained expression of these markers at E12.5 (Figure 1A). Expression of *TrkC* in the precursors started to be downregulated at E14.5 and was largely mutually exclusive with RET and TRKA in sympathetic neurons at E15.5 (Supplementary Figure S1).

Analysis of P5 SG revealed that VAChT$^+$ neurons segregated with RET, PRPH, Vasoactive Intestinal Peptide (VIP) and Somatostatin (SST), while *TrkA* expression was initiated in VMAT2$^+$ neurons (Figure 1B). These neurons also contained DBH and some, neuropeptide Y (NPY) (Figure 1B). Quantification of the number of neurons expressing *Vmat2*, *TrkA*, *VAChT* and *Ret* throughout development was performed to resolve the exact developmental sequence of sympathetic neuron diversification (Figures 1C–F). While RET was rapidly extinguished in most neurons between E14.5 and E15.5, TRKA$^+$ neurons first appeared at E14.5 and increased progressively until E18.5. Approximately half of the TRKA$^+$ neurons at E14.5 were RET$^+$/TRKA$^+$ hybrid after which RET was rapidly segregated, and only 2.2 ± 0.6% of the TRKA$^+$ neurons remained as a hybrid population at P5 (Figure 1E). Also *Vmat2* and *VAChT*, expressed in nearly all precursors at early stages, rapidly segregated between E14.5 and E15.5 (Figures 1D and F). Hence, already at E18.5 a noradrenergic TRKA$^+$/VMAT2$^+$/RET$^-$ and cholinergic VAChT$^+$/RET$^+$/PRPH$^+$ population were nearly completely segregated by a mechanism involving extinction of TRKC in most segregated neurons, and in noradrenergic neurons maintenance of TH, VMAT2 and DBH, induction of TRKA combined with extinction of ChAT, VAChT and PRPH while cholinergic neurons emerged through maintenance of ChAT, VAChT, RET and PRPH and extinction of TH, VMAT2 and DBH.

To directly prove that both noradrenergic and cholinergic sympathetic neurons arise from a common pool of RET$^+$ precursors, genetic-based cell lineage tracing experiments were performed using mice heterozygous for an inducible CRE (CreERT2) in the *Ret* locus (*Ret*^{ERT2}) (Luo *et al*, 2009) crossed to the *Gt(ROSA)26*$^{tm9(CAG\text{-}tdTomato)}$ strain (*R26*^{TOMATO}). Tamoxifen was administered at E11.5 and the animals were sacrificed at E18.5 for analysis. Analysis of TOMATO$^+$ cells expressing *TrkA*, *Ret* or both, revealed 66.4, 25.7 and 7.9% of traced cells, respectively (Figures 1G and H). This shows that early RET$^+$ sympathetic precursor cells are the cellular origin of both noradrenergic and cholinergic sympathetic neurons. Taken together, the above results suggest a defined organization of segregation which is intimately associated with expression of *TrkA* and *Ret* from an early precursor population.

Acquisition of Hmx1 expression defines the major population of noradrenergic neurons

An *Hmx1* mouse allele containing LacZ fused to the start codon of *Hmx1* (*Hmx1*^{LcZ} mice, Supplementary Figure S2) was used for β-galactosidase immunohistochemistry to quantify *Hmx1* expressing neurons during sympathetic neuron differentiation. HMX1 first appeared in very few cells in the ganglia at E13.5, which increased in numbers until E18.5 and remained at a similar level at P5 (Figure 2A). HMX1 was strongly associated with *TrkA* expressing neurons throughout development. However, prior to *TrkA* expression, that is, at early stages such as E13.5–E14.5, *Hmx1* was initiated in RET$^+$ precursors. *Ret* was then rapidly extinguished in HMX1$^+$ neurons, since already at E15.5, *Ret* and *Hmx1* expression were largely mutually exclusive (Figure 2B). *Hmx1* expression clearly preceded both the upregulation of *TrkA* and the downregulation of *Ret* (Figures 2A, insets and C). Consistently, expression of *Hmx1* was initiated in TRKC$^+$ precursors at E13.5 fated to the noradrenergic lineage of sympathetic neurons (Supplementary Figure S3). In agreement with this, *Hmx1* was expressed in VMAT2$^+$ neurons but was never present in RET$^+$/VAChT$^+$ neurons at E15.5 (Supplementary Figure S4A and B) and P5 (Supplementary Figure S5K). A proposed hierarchical organization of the development of sympathetic subtypes is shown in Figure 2D.

Hmx1 consolidates the sympathetic noradrenergic fate

The strict relation of HMX1 to the TRKA$^+$/VMAT2$^+$/RET$^-$ neuronal population led us to generate an *Hmx1* conditional null mutant allele lacking the homeobox domain and the 3′ untranslated region (UTR) (Figure 3A; Supplementary Figure S5A and G). The conditional allele was crossed to *Wnt1-Cre* mice to delete *Hmx1* in neural crest-derived cells, including sympathetic neurons (*Hmx1*$^{fl/fl}$*;Wnt1-Cre* mice). *In situ* hybridization for *Hmx1* confirmed the efficient deletion of *Hmx1* in sympathetic neurons in the *Hmx1*$^{fl/fl}$*; Wnt1-Cre* mouse strain (Supplementary Figure S5H).

Expression of *TrkA* was markedly absent in the mutant at E15.5, the critical stage for acquisition of *TrkA* expression (46.5 ± 2.5% positive neurons in wild-type and 9.9 ± 1.0% positive neurons *Hmx1*$^{fl/fl}$*;Wnt1-Cre* mice) and was not recovered by P0 (88.1 ± 1.9 wild-type and 28.3 ± 2.0% *Hmx1*$^{fl/fl}$*;Wnt1-Cre* mice) (Figure 3B and C). Analysis of RET and TRKA double-stained neurons from P0 *Hmx1*$^{fl/fl}$*; Wnt1-Cre* mice showed that most or all of the few neurons expressing *TrkA* independent of *Hmx1* were hybrid RET$^+$/TRKA$^+$ neurons (Figure 3B). While some markers, including DBH and VMAT2 (Supplementary Figure S5J), were not regulated by HMX1 at P0, HMX1 was found to be critical for the expression of the noradrenergic neurotransmitter phenotype, since the number of TH$^+$ neurons was also dramatically reduced at P0, from 93.3 ± 0.8% in wild-type mice to 27.9 ± 2.7% in *Hmx1*$^{fl/fl}$*;Wnt1-Cre* mice (Figure 3B). Interestingly, *Th* was expressed at E15.5 in similar number of cells in *Hmx1*$^{fl/fl}$*;Wnt1-Cre* mice as in control (*Hmx1*$^{fl/fl}$) mice, although at lower levels (Figure 3C). This shows that HMX1 is necessary around E15 to consolidate a noradrenergic phenotype in precursors that segregate into noradrenergic sympathetic neurons by mechanisms of induction and maintenance of noradrenergic lineage-specific genes *TrkA* and *Th*, respectively. Although neuronal numbers were increased in *Hmx1*$^{-/-}$ mice at P0 (Supplementary Figure S5I), arrector

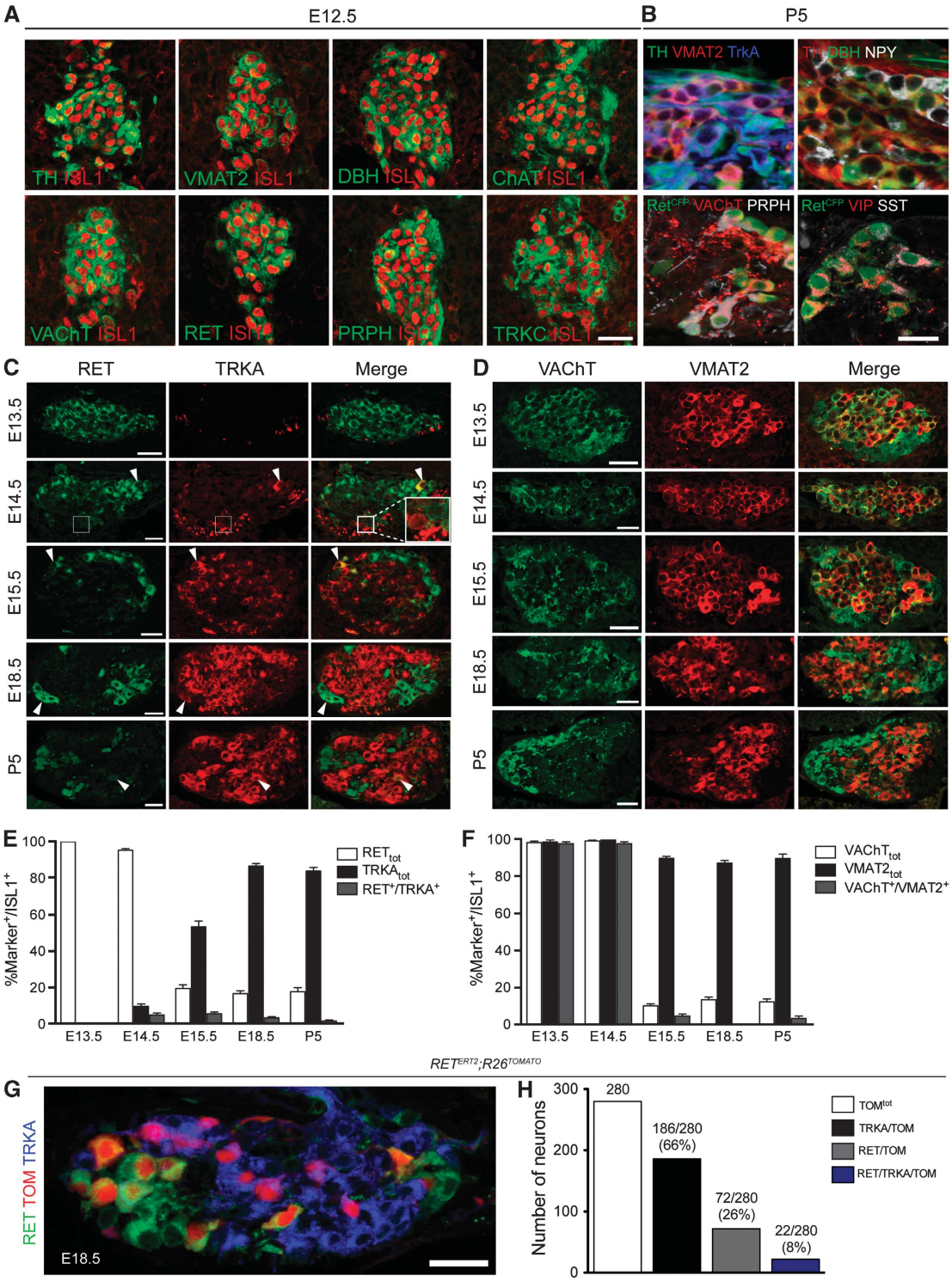

Figure 1 Sympathetic precursors of hybrid phenotype diversify into distinct neurotransmitter subtypes. (**A**) E12.5 sympathetic precursors display a mixed phenotype, expressing genes associated with both noradrenergic and cholinergic sympathetic neuron phenotypes. Double immunostaining for indicated proteins on E12.5 sympathetic ganglia (SG) sections. Section for VMAT2 is the same as VAChT, with red channel converted to green. (**B**) Association of markers with noradrenergic and cholinergic sympathetic neurons at P5. Note co-expression of noradrenergic (TH, VMAT2, DBH, NPY and TRKA, upper panels) and cholinergic (RET, VAChT, PRPH, VIP and SST, lower panels) markers. (**C**–**F**) Diversification of the sympathetic lineage as revealed by *Ret*, *TrkA*, *VAChT* and *Vmat2* expression during development. (**C**, **D**) Double immunostaining for RET/TRKA (**C**) and VAChT/VMAT2 (**D**) on SG sections from indicated ages. Note the onset of *TrkA* expression at E14.5 and the concomitant downregulation of *Ret* (**C**, inset) and *VAChT* (**D**). Sporadic hybrid neurons expressing both *Ret* and *TrkA* are observed until P5 (**C**, arrowheads). (**E**, **F**) Quantification of (**C**) and (**D**). Results are represented as mean ± s.e.m. $n = 10$–26 ganglia from at least two animals for each stage. (**G**, **H**) E11.5 RET^+ SG neurons contribute to the $TRKA^+$, RET^+ and hybrid $RET^+/TRKA^+$ neurons at E18.5. (**G**) Double immunostaining for RET and TRKA on SG sections at E18.5. Note $TOMATO^+$ cells (TOM) in both the RET^+ and $TRKA^+$ lineages. (**H**) Quantification of (**G**). Scale bar in all images represents 50 μm.

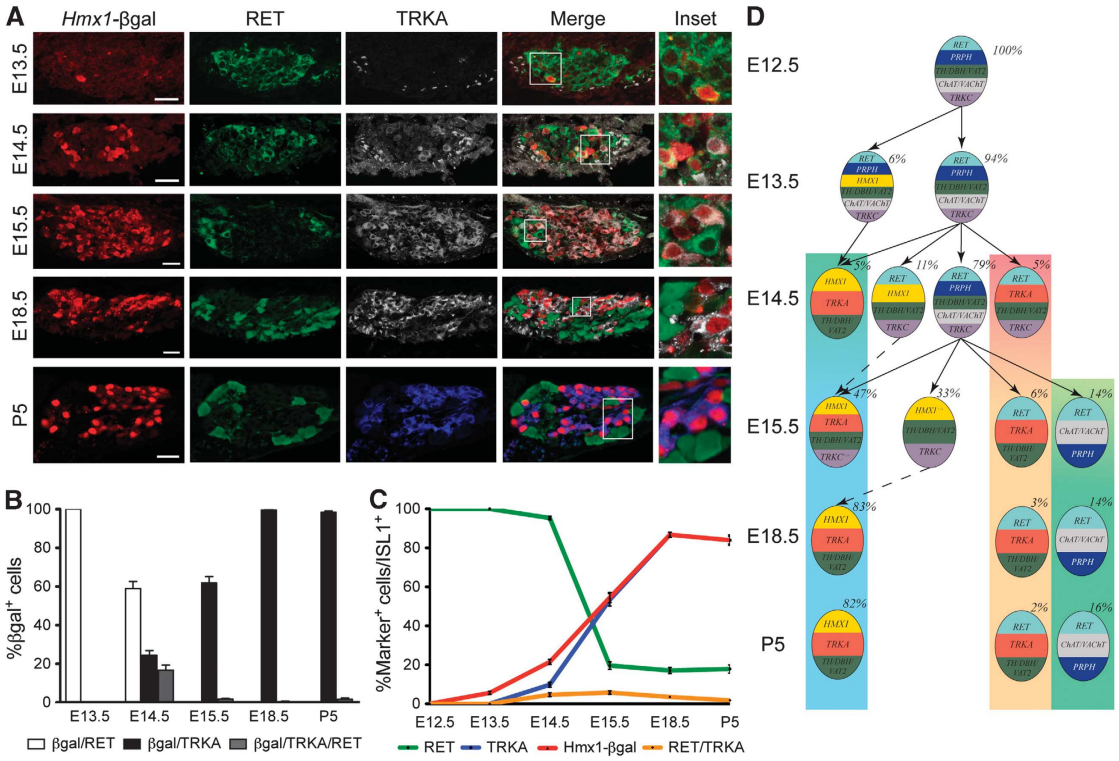

Figure 2 Expression of the homeobox transcription factor *Hmx1* defines the major population of noradrenergic neurons. (**A**) Triple immunostaining for *Hmx1*-βgal, RET and TRKA on SG section of indicated ages in $Hmx1^{LcZ/+}$ or $Hmx1^{LcZ/+}$;$RET^{CFP/+}$ mice. Note the onset of *Hmx1* expression, revealed by βgal expression, at E13.5 in RET^+ neurons (inset). At E14.5, $\beta gal^+/TRKA^+/RET^-$, $\beta gal^+/TRKA^-/RET^+$ and $\beta gal^+/RET^+/TRKA^+$ (inset) neurons are observed. At E15.5, most neurons co-express βgal and *TrkA* (inset) while RET^+ neurons are βgal^-. At E18.5 and P5, nearly all neurons in the ganglion are either $\beta gal^+/TRKA^+$ or only RET^+ (inset). Scale bar in all images represents 50 μm. (**B**) Quantification of (**A**). Results are represented as mean ± s.e.m. $n = 6$–26 ganglia from at least 2 animals for each stage. (**C**) Graph showing proportion of RET^+, βgal^+, $TRKA^+$ and $RET^+/TRKA^+$ neurons in $ISL1^+$ neurons throughout development. Note *Hmx1* preceding *TrkA* expression by about 1 day. (**D**) Schematic representation of the different main lineages with indicated percent of their contribution to all neurons at each stage during the course of sympathetic neuron differentiation in mouse. *Hmx1* expression predefines a noradrenergic fate.

pili muscle and cutaneous blood vessel innervation by $PGP9.5^+$ and TH^+ noradrenergic fibres was markedly reduced at P19 (Supplementary Figure S7), consistent with a requirement of NGF signalling via TRKA for a full innervation of target tissues. Analysis of RET^+ neurons in $Hmx1^{fl/fl}$;*Wnt1-Cre* mice revealed a complete failure of *Ret* suppression, as most or all of the sympathetic neurons expressed *Ret* at P0 (Figure 3B). Similar results were obtained when analysing E15.5 $Hmx1^{fl/fl}$;*Wnt1-Cre* mice (Figure 3B and C). In addition to *Ret*, *Vip* and *Sst*, normally expressed in the RET^+ cholinergic sympathetic neurons, also failed to be repressed in the noradrenergic sympathetic neurons (Figure 3B), while *ChAT* and *VAChT* were unaffected (Supplementary Figure S5J). In $Hmx1^{LcZ/fl}$;*Wnt1-Cre mice*, which allow monitoring of cells that should normally express *Hmx1*, the absence of HMX1 led to *Ret* expression in $\beta\text{-gal}^+$ cells while, in control animals, *Ret* and β-*gal* expression was mutually exclusive (Supplementary Figure S5K). Thus, this conclusively shows a requirement for HMX1 for suppression of cholinergic traits in noradrenergic sympathetic neurons.

Th expression is governed by PHOX2B and HAND2 in sympathetic precursors, consistently, in *Phox2b* and *Hand2* null mutant mice, *Th* expression is absent in sympathetic precursors (Pattyn *et al*, 1999; Morikawa *et al*, 2007). $Hmx1^{fl/fl}$;*Wnt1-Cre* mice did not display any deficits of *Phox2a/b* expression (Figure 3C), indicating that early expression of *Th* in sympathetic precursors is governed by these transcription factors independently of HMX1. Hence, although the previously identified gene-regulatory network is sufficient for inducing a sympathetic lineage with noradrenergic traits, consolidation of this phenotype and repression of other fates within the major population of noradrenergic sympathetic neurons requires HMX1.

TrkC biases segregation into cholinergic sympathetic neurons

TrkC is expressed in early sympathetic precursors (Ernfors *et al*, 1992). We find that *Hmx1* is initiated within the $TRKC^+$ precursors at E13.5 (Supplementary Figure S3), but is largely mutually exclusive with HMX1 at E15.5 through an extinction of *TrkC* expression in neurons attaining HMX1 (Figure 4A and B), consistent with the findings that *TrkC* is expressed in precursors, since $TRKC^+$ neurons were rarely positive for RET or TRKA at E15.5 (Supplementary Figure S1). $TrkC^{-/-}$ and $TrkC^{-/-}$;$Bax^{-/-}$ mice were analysed to address the role of TRKC during diversification of sympathetic neurons into distinct types. $TrkC^{-/-}$;$Bax^{-/-}$ mice were used to ascertain analysis of survival-independent functions of TRKC (Patel *et al*, 2000). Lack of TRKC led to a marked de-repression of *Hmx1* expression (Figure 4C). Consistently, mice lacking TRKC displayed a large reduction in RET^+ neurons at E15.5 ($TrkC^{-/-}$;$Bax^{-/-}$) and E18.5 ($TrkC^{-/-}$) (Figure 4D, F and G). The reduction in RET^+ neurons was paralleled by an increase in $TRKA^+$ neurons (Figure 4D, F and G).

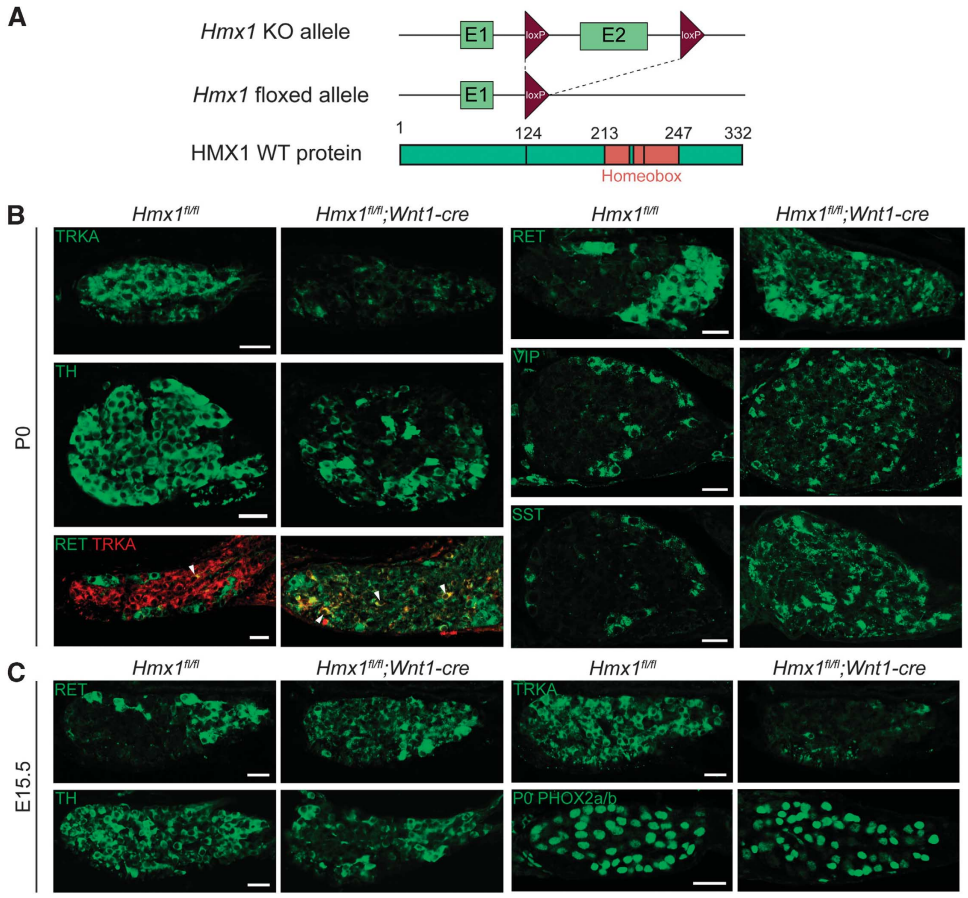

Figure 3 Consolidation of noradrenergic and suppression of cholinergic traits by *Hmx1*. (**A**) Schematic illustration of the *Hmx1* allele in conditional mutant mice. Exon 2 encoding amino acids 124–332 of *Hmx1*, including the homeobox domain, was flanked by LoxP sites. (**B**, **C**) Immunostaining for TRKA, RET, TH, VIP and SST on SG sections from control and $Hmx1^{fl/fl}$;*Wnt1-Cre* animals at P0 (**B**) and for RET, TRKA and TH at E15.5 (**C**). (**B**) In the absence of HMX1, the noradrenergic genes *TrkA* and *Th* are markedly decreased, while cholinergic-associated genes including *Ret*, *Vip* and *Sst* fail to be repressed in P0 mutant animals. *Phox2a/b* expression is unchanged at P0 (**C**). Double staining for RET and TRKA at P0 reveals that remaining $TRKA^+$ neurons fail to repress *Ret* (**B**, arrowheads). (**C**) *Ret* downregulation and *TrkA* induction fail as early as E15.5 in the absence of HMX1. Furthermore, *TH* expression levels are decreased in $Hmx1^{fl/fl}$;*Wnt1-Cre* animals at E15.5. Scale bar in all images represents 50 μm.

This switch in receptor expression represented a change in fate, since $ChAT^+$ neurons decreased while TH^+ neurons increased (Figure 4E and G) to a similar extent as RET^+ and $TRKA^+$ neurons. Hence, a de-repression of *Hmx1* in $TrkC^{-/-}$;$Bax^{-/-}$ mice leads to induction of *TrkA* and repression of *Ret* that participate in the failure of diversification of cholinergic sympathetic neurons in the absence of *TrkC*.

A Ret-dependent segregation of sympathetic neurotransmitter fates

In $Ret^{-/-}$ mice, *ChAT* and *VAChT* fail to be expressed at E16 (Burau *et al*, 2004). Hence, the marked loss of RET^+ and $ChAT^+$ neurons and increase in $TRKA^+$ and TH^+ neurons in mice lacking TRKC suggest that TRKC may bias a cholinergic fate in precursors via its regulation of *Ret*. In this case, *Hmx1* expression is also expected to be de-repressed in $Ret^{-/-}$ mice. Analysis of β-*gal* expression from the Hmx1 locus in $Ret^{CFP/CFP}$;$Hmx1^{LcZ/+}$ mice revealed a near three-fold increase in *Hmx1* expressing neurons at E14.5 (Figure 5B; Supplementary Figure S6A) and an around 1.4-fold increase at E15.5 (Figure 5A and B) as compared to control $Ret^{CFP/+}$;$Hmx1^{LcZ/+}$ mice. To address whether the increases in $HMX1^+$ cells represented only precocious expression, or also expression in neurons which normally do not express it, we analysed co-localization of RET with TRKC or HMX1 in control and RET-deficient mice. For this purpose, we used the Ret^{CFP} allele that expresses CFP from the null *Ret* locus and therefore can be used to identify cells that normally should have expressed *Ret*. Control $Ret^{CFP/+}$;$Hmx1^{LcZ/+}$ and *Ret* null $Ret^{CFP/CFP}$;$Hmx1^{LcZ/+}$ mice were analysed at E15.5. In control mice, *Hmx1* and *Ret* expression was largely mutually exclusive. In contrast, in the absence of RET, a large number of neurons that normally should express *Ret* had initiated ectopic *Hmx1* expression (Figure 5M). Therefore, an absence of RET leads to both precocious and ectopic expression of *Hmx1* in some precursor cells. *TrkA* was also precociously expressed at E14.5 and the increase in $TRKA^+$ neuronal numbers was similar to $HMX1^+$ neuron increase at both E14.5 and E15.5, with a full co-localization of HMX1 and TRKA in the neurons (Figure 5C and D; Supplementary Figure S6A). Absence of RET signalling not only led to an increase in noradrenergic phenotypes, but also to a partial or near complete loss of cholinergic phenotypes, including VIP, SST, ChAT and VAChT (Figure 5G–L; Supplementary Figure S6B).

A small increase in $TRKC^+$ neurons was observed in the absence of RET (Figure 5E and F). In $Ret^{CFP/CFP}$ null mutant mice, large numbers of cells that normally should express *Ret* displayed *TrkC* expression (Figure 5N), likely reflecting a

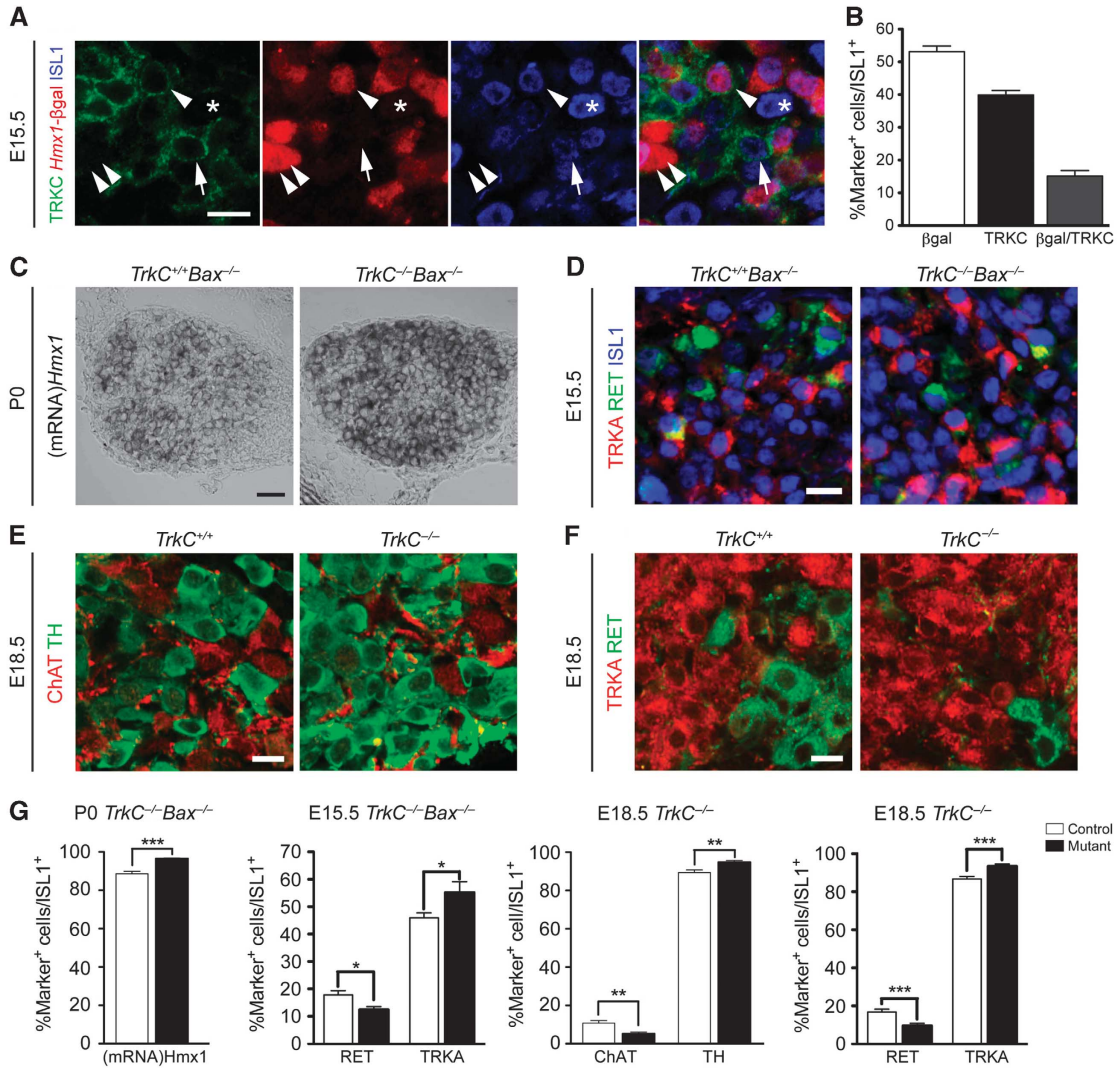

Figure 4 A failure of *Hmx1* repression and development of cholinergic neurons in mice lacking *TrkC*. (**A**) Triple immunostaining for TRKC, *Hmx1*-βgal and ISL1 on SG section of E15.5 $Hmx1^{LcZ/+}$ embryos. Note $\beta gal^+/TRKC^+$ neurons (arrowheads), $\beta gal^+/TRKC^-$ (double arrowheads), $\beta gal^-/TRKC^+$ (arrows) and $\beta gal^-/TRKC^-$ (asterisk) neurons in the E15.5 SG. Scale bar represents 20 μm. (**B**) Quantification of (**A**). (**C**) *In situ* hybridization for (mRNA) *Hmx1* on SG section of a P0 $TrkC^{-/-};Bax^{-/-}$ animal. Note increased expression of *Hmx1* mRNA in the absence of TRKC. Scale bar represents 50 μm. (**D**) Triple immunostaining for TRKA, RET and ISL1 on SG sections of E15.5 WT and $TrkC^{-/-};Bax^{-/-}$ embryos. Note the decreased and increased proportion of RET^+ neurons and $TRKA^+$ neurons, respectively, in the absence of TRKC. Scale bar represents 20 μm. (**E**, **F**) Double immunostaining for TH and ChAT (**E**) and for TRKA and RET (**F**) on SG sections of E18.5 WT and $TrkC^{-/-}$ embryos. Note the decreased number of $ChAT^+$ (**E**) and RET^+ (**F**) neurons. Scale bar represents 20 μm. (**G**) Quantification of (**C**–**F**). Results are represented as mean ± s.e.m. $n = 9$–26 ganglia from at least 2 animals for each stage. Statistical significance was determined using Student's *t*-test. $^*P<0.05$, $^{**}P<0.01$, $^{***}P<0.0001$.

delayed commitment of some precursors at E15.5 in the absence of RET. Combined, these data suggest that in the absence of RET, following a short delay in specification of $TRKC^+$ precursors, *Hmx1* is de-repressed and cholinergic markers including VIP, SST, ChAT and VAChT fail to be maintained, these neurons attain ectopic *TrkA* expression and ultimately change fate from cholinergic to noradrenergic lineage of sympathetic neurons.

By microarray experiments and confirmative RT–PCR, expression of T-cell leukaemia homeobox 3 (*Tlx3*) has been shown to increase in cultures of E12 chick sympathetic chain grown in the presence of pro-cholinergic differentiation factors (Apostolova *et al*, 2007). Immunohistochemical staining for TLX3 revealed its expression in nearly all precursors at E13.5 and became largely mutually exclusive with HMX1 already at E15.5 by a downregulation in many neurons (Figure 6A). Most $TLX3^+$ cells were $VAChT^+$ at E15.5, although some still expressed TH, while at P60 TLX3 was confined exclusively to $VAChT^+$ neurons (Figure 6B). *Tlx3* failed to be repressed in $Hmx1^{fl/fl};Wnt1\text{-}Cre$ mice at E15.5 and P0 and all $TLX3^+$ cells also stained for RET (Figures 6C and D). A direct role of HMX1 in repression of *Tlx3* in the cholinergic lineage of sympathetic neurons was established by analysis of $Hmx1^{LcZ/fl}$; *Wnt1-Cre* mice at P5 in which β-galactosidase is expressed in *Hmx1* null cells that normally should have expressed *Hmx1*. In contrast to control ($Hmx1^{lcZ/fl}$) mice, *Tlx3* failed to be repressed in HMX1-deficient neurons fated to the noradrenergic lineage, as revealed by co-localization of β-galactosidase and TLX3 in $Hmx1^{LcZ/fl};Wnt1\text{-}Cre$ mice (Figure 6E). These results show that *Tlx3*, initially expressed in all precursors, becomes restricted to cholinergic neurons via a mechanism that

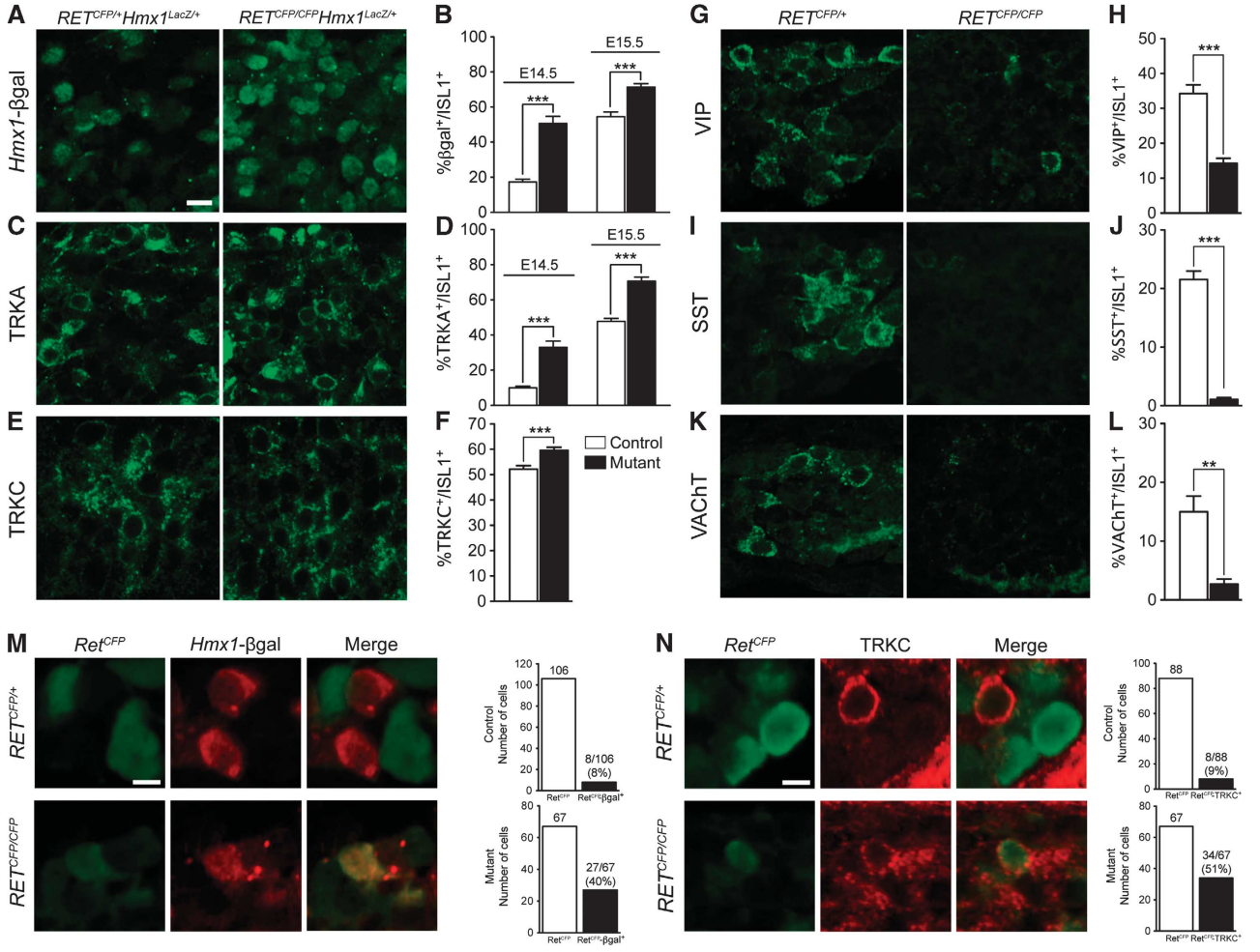

Figure 5 A critical role of RET for suppression of noradrenergic and maintenance of a cholinergic phenotype. (**A**–**L**) Expression of *Hmx1*-βgal (**A**, **B**), *TrkA* (**C**, **D**), *TrkC* (**E**, **F**), *Vip* (**G**, **H**), *Sst* (**I**, **J**) and *VAChT* (**K**, **L**) on SG sections from E15.5 control and *Ret* mutant mice (i.e., $Ret^{CFP/CFP}$) mice, as indicated. (**B**, **D**, **F**, **H**, **J** and **L**) Quantifications of (**A**, **C**, **E**, **G**, **I** and **K**). Results are represented as mean ± s.e.m. $n = 10$–20 ganglia from at least 2 animals for each stage. Scale bar represents 50 μm. Statistical analysis was performed using Student's *t*-test. $^{**}P<0.01$, $^{***}P<0.0001$. (**M**, **N**) Change of fate of RET^{+} neurons determined by identification of cells that normally should express *Ret* using a Ret^{CFP} knock-in allele and staining with an anti-GFP antibody that detects CFP in E15.5 RET^{CFP} embryos. (**M**) Neurons normally expressing *Ret* fail to suppress *Hmx1* in E15.5 mice as seen by double immunostaining for CFP and *Hmx1*-βgal on SG sections from E15.5 $Ret^{CFP/+}$ and $Ret^{CFP/CFP}$ embryos. Note expression of *Hmx1* and CFP being almost mutually exclusive in the control while CFP^{+} neurons express βgal in $Ret^{CFP/CFP}$ mice. Quantifications are presented on the right. Numbers above bars indicate number of cells positive for the marker. $n = 10$–20 ganglia. Scale bar represents 10 μm. (**N**) Note almost mutually exclusive expression of *CFP* and *TrkC* in control ($Ret^{CFP/+}$) mice and a failure of suppression of *TrkC* in cells which normally express *Ret* in *Ret* mutant ($Ret^{CFP/CFP}$) mice. Quantifications are presented on the right. Numbers above bars indicate number of cells positive for the marker. $n = 10$–20 ganglia. Scale bar represents 10 μm.

involves its repression by HMX1 in neurons fated to the noradrenergic lineage.

Discussion

Here, we delineate the hierarchical cascade of sympathetic neuron diversification and identify how a transcriptional regulatory mechanism and neurotrophic tyrosine kinase receptors coordinate specification of the sympathetic lineage in the trunk. Although a transcriptional gene-regulatory network fating the sympathetic lineage and noradrenergic phenotype in precursors has previously been described, our study demonstrates that these early precursors display a mixed noradrenergic and cholinergic phenotype. The hybrid precursors with mixed phenotype segregate into distinct sympathetic lineages in a process starting around E13.5. We found that initiation of *Hmx1* expression in precursors plays a critical role for the expression of *TrkA* and for the consolidation of a noradrenergic fate, while TRKC and RET determine a cholinergic phenotype. Together, our results unveil an intricate developmental process during specification of sympathetic neurons in which tyrosine kinase receptors and transcriptional activators, in cross-regulatory interactions, determine the ultimate function of sympathetic neuronal subtypes. A schematic representation depicting the gene-regulatory interactions determining sympathetic subtypes is shown in Figure 6F and G.

Induction of the sympathetic fate and its relation to diversification and consolidation of neurotransmitter phenotypes

An important aspect of these results is the relation of identified factors to the previously much studied gene-regulatory network inducing and defining the sympathetic lineage

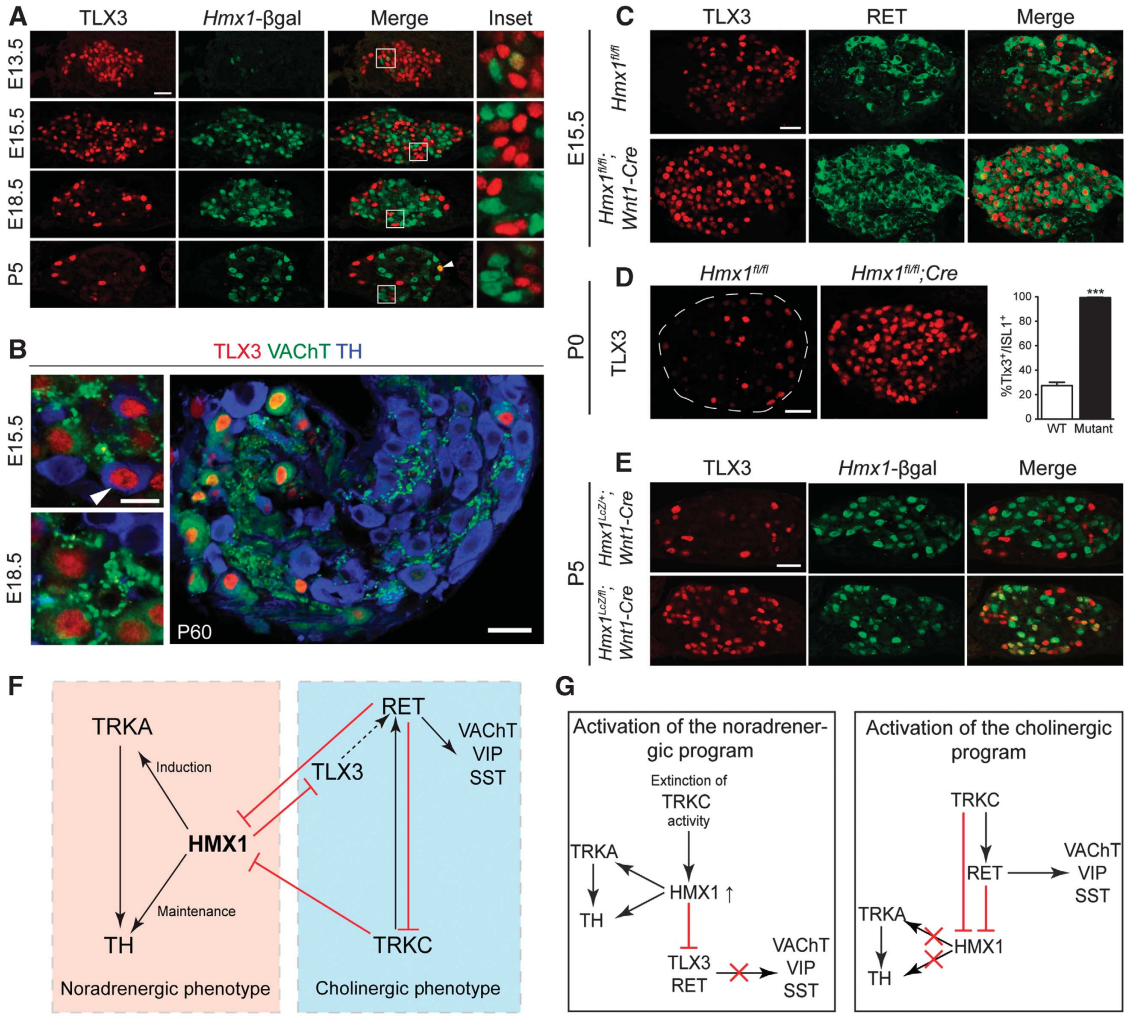

Figure 6 TLX3 segregates in the RET$^+$/VAChT$^+$ neurons and its expression is regulated by HMX1. (**A**) Double immunostaining for TLX3 and *Hmx1*-βgal on SG section in *Hmx1*$^{LcZ/+}$ mice of indicated ages. At E13.5, note emergence of *Hmx1* expression in TLX3$^+$ neurons and downregulation of *Tlx3* expression in these neurons (inset). At E15.5, E18.5 and P5, expression of *Hmx1* and *Tlx3* becomes almost mutually exclusive (insets) although rare, TLX3$^+$/HMX1$^+$ neurons are present even at late stages (P5, arrowhead). (**B**) Triple immunostaining for TLX3, VAChT and TH on SG section in wild-type mice of indicated ages. Note expression of *Tlx3* in some TH$^+$ neurons at E15.5 (arrowhead) but complete segregation in VAChT$^+$ neurons at later embryonic stages. (**C**, **D**) Double immunostaining for TLX3 and RET on SG sections from control and *Hmx1*$^{fl/fl}$*;Wnt1-Cre* animals at E15.5 (**C**) and for TLX3 at P0 (**D**). Note de-repression of *Tlx3* and *Ret* expression in neurons lacking HMX1 at both stages. (**E**) Double immunostaining for TLX3 and *Hmx1*-βgal on SG section from control (*Hmx1*$^{LcZ/+}$*;Wnt1-Cre*) and mutant (*Hmx1*$^{LcZ/fl}$*;Wnt1-Cre*) animals at P5. Note *Hmx1* expression mutually exclusive with *Tlx3* in control (upper panel) but not in mutant SG (lower panel) showing that in the absence of HMX1, many of the neurons that normally express *Hmx1* (i.e., *Hmx1*-βgal$^+$ neurons) acquire *Tlx3* expression. Scale bar represents 50 μm. (**F**) Schematic representation of gene-regulatory interactions determining noradrenergic and cholinergic sympathetic subtypes. (**G**) Schematic representation showing the temporal activation of the genetic program defining the noradrenergic and cholinergic differentiation programs. Arrows show positive regulation and red lines show negative regulation.

during development. The sympathetic lineage is induced in NCCs migrating in the ventral migratory pathway. BMPs are expressed in the dorsal aorta, and as NCCs reach the vicinity of the dorsal aorta, BMPs induce expression of a complex transcriptional regulatory unit including *Mash1* (Guillemot *et al*, 1993; Hirsch *et al*, 1998; Lo *et al*, 1998), basic helix-loop-helix (bHLH), DNA binding protein *Hand2* and *Phox2a* and *Phox2b* (Morin *et al*, 1997; Pattyn *et al*, 1997, 1999; Lo *et al*, 1999; Stanke *et al*, 1999). Transcription of *Th* and *Dbh*, encoding enzymes in noradrenalin synthesis, is regulated by *Phox2* proteins and enhanced by HAND2 (Xu *et al*, 2003), which is also critical for the noradrenergic fate and proliferation *in vivo* (Goridis and Rohrer, 2002; Howard, 2005; Apostolova and Dechant, 2009). It is interesting that we find a failure of maintenance of *Th* expression in newborn *Hmx1*$^{fl/fl}$*;Wnt1-Cre* mice without any alterations in *Phox2a/b* expression. Our results show that PHOX2A/B and HAND2 are sufficient for *Th* expression independently of HMX1 at early stages, while a defining aspect during diversification is a change in requirements. During diversification, *Hmx1* expression becomes critical for the maintenance of the noradrenergic phenotype as defined by expression of the rate-limiting enzyme in noradrenalin synthesis, TH.

One critical underlying mechanism that may participate in the change of requirements might be the extinction of TRKC activity. We find that TRKC is expressed in all hybrid noradrenergic/cholinergic precursors but is largely downregulated as these diversify into distinct types. In *TrkC*$^{-/-}$ mice, *Hmx1*-mRNA levels are markedly elevated, showing that TRKC is suppressing *Hmx1* expression. Therefore, reduced levels of TRKC activity in hybrid precursors might be a requirement for onset of *Hmx1* expression. BMP2 has been

shown to robustly upregulate *TrkC* expression in cultured E15 sympathetic neurons (Zhang *et al*, 1998). Hence, BMP signalling may not only be critical for inducing the sympathetic lineage at early stages, but a temporal window of BMP with declining levels starting around E13 could also initiate diversification in the sympathetic lineage, via an insufficient sustainment of *TrkC* expression and activity. Although most targets eventually receive some sympathetic innervation, proximal axon extension requires the TRKC ligand, NT3 (ElShamy *et al*, 1996; Francis *et al*, 1999; Kuruvilla *et al*, 2004). While NT3 does not mediate sympathetic precursor survival, the 50% loss of sympathetic neurons in $Nt3^{-/-}$ mice coincides at a later stage in development with the period of excessive neuronal loss in $Ngf^{-/-}$ mice (Wyatt *et al*, 1997; Francis *et al*, 1999; Kuruvilla *et al*, 2004). At these late embryonic stages, we find that *TrkC* is largely downregulated in sympathetic neurons consistent with the interpretation that a deficit in early axon growth leads to a subsequent impairment in attaining target-derived NGF that is required for neuronal survival (Glebova and Ginty, 2005). Here, we find that in addition to affecting proximal axon growth, TRKC plays an important role in sympathetic neuron diversification by regulating the neurotransmitter fate and in its absence, a switch in fate from cholinergic to noradrenergic neurons is observed.

Specification of noradrenergic neurons

Onset of *Hmx1* expression in sympathetic precursors is critical for several, but not all, defining aspects of development of noradrenergic sympathetic neurons. First, while PHOX2AB/HAND2 is required for initiation of *Th* expression in hybrid precursors, HMX1 is necessary for its maintenance in noradrenergic sympathetic neurons as these diversify from sympathetic precursors. This requirement is clearly an independent mechanism from *Phox2ab/Hand2* induction, since *Dbh* expression, which also requires PHOX2AB/HAND2, is not affected by *Hmx1* deficiency. Furthermore, the onset of *Hmx1* expression is critical for expression of *TrkA* in noradrenergic sympathetic neurons. *TrkA* expression is defining for these neurons, as signalling through this receptor plays fundamental roles in development of the noradrenergic sympathetic nervous system. NGF promotes extensive neurite growth and hypertrophy of sympathetic neurons (Levi-Montalcini, 1987), an activity critical for final sympathetic target innervation but not proximal growth *in vivo* (Glebova and Ginty, 2004). TRKA signalling is also critical for survival of sympathetic neurons and in its absence essentially no noradrenergic sympathetic neurons remain, as revealed in mice lacking TRKA or NGF ($TrkA^{-/-}$ and $Ngf^{-/-}$ mice) (Crowley *et al*, 1994; Smeyne *et al*, 1994; Fagan *et al*, 1996b). NGF signalling via TRKA leads to robust upregulation of *Th* expression in cultured sympathetic neurons (Otten *et al*, 1978; Brodski *et al*, 2000). A dependence on *Hmx1* expression for maintenance of *Th* expression in the noradrenergic sympathetic lineage and for consolidation of the noradrenergic phenotype may therefore be a result of direct and/or indirect activity of HMX1 via its regulatory activities on *TrkA* expression. Thus, it is possible that HMX1-induced *TrkA* expression allows for TRKA signalling, which maintains *Th* expression in the noradrenergic sympathetic neuronal subtypes. The deficits of *TrkA* expression and specification of the noradrenergic phenotype of $Hmx1^{fl/fl}$;*Wnt1-Cre* mice resulted in a marked reduction of innervation of the arrector pili muscle and subcutaneous blood vessels, consistent with the critical role of *TrkA* for target innervation. Our results on cell counts revealed an unexpected increase in trunk sympathetic neurons in the $Hmx1^{fl/fl}$;*Wnt1-Cre* mice. One possibility is that a remaining low level of *TrkA* is sufficient for neuronal survival. This is consistent with that despite that both heterozygous mice for *Ngf* and *TrkA* display reduced levels of gene expression, $Ngf^{+/-}$ mice but not $TrkA^{+/-}$ mice display excessive neuronal loss (Brennan *et al*, 1999; Ghasemlou *et al*, 2004). Hence, TrkA does not appear to be limiting during development. Another possibility is that in the absence of HMX1, the altered phenotype (i.e., for instance massive increase in *Ret* expression) allows for TRKA-independent survival.

HMX1 is not only important for induction of *TrkA* and maintenance of *Th*, but also for repression of phenotypic characteristics associated with the alternative, cholinergic, fate. In $Hmx1^{fl/fl}$;*Wnt1-Cre* mice *Ret*, *Vip* and *Sst* are broadly expressed in neurons throughout the ganglion, representing a failure of suppression of their expression in the noradrenergic lineage, due to *Ret* failing to be repressed in neurons that normally should have expressed *Hmx1* (as revealed using $Hmx1^{LcZ/fl}$;*Wnt1-Cre mice*). The failure of suppression of *Ret* in $Hmx1^{fl/fl}$;*Wnt1-Cre* mice explains the persistent expression of *Vip* and *Sst* in these mice, since both these genes are induced by RET signalling. Hence, HMX1 defines a noradrenergic fate by sustaining the noradrenergic sympathetic phenotype already present in precursors and by eliminating gene expression associated with the alternative cholinergic phenotype.

Specification of cholinergic neurons

Cholinergic sympathetic innervation of sweat glands and periosteum in rodents have been shown to emerge postnatally from noradrenergic innervation as a result of a change in neurotransmitter phenotype from noradrenergic to cholinergic by soluble signals (Schotzinger *et al*, 1994; Francis and Landis, 1999). Our results show that TRKC directly affects the fate of sympathetic precursors by promoting development along the cholinergic sympathetic fate. It is unclear if this role of TRKC is ligand dependent or ligand independent. An increased cell death reported in $Nt3^{-/-}$ but not in $TrkC^{-/-}$ mice (Fagan *et al*, 1996a; Tessarollo *et al*, 1997) and no additional loss in $Nt3^{-/-}/Ngf^{-/-}$ compound mutant mice as compared to $Ngf^{-/-}$ mice (Francis *et al*, 1999) indicate that the early role of NT3 for proximal axon growth that later results in an NGF-deprivation induced death caused by failure of target innervation is mediated via TRKA interactions. This conclusion concur with that NT3 can signal via both TRKC and TRKA in sympathetic neurons (Davies *et al*, 1995). Although previous studies have not addressed deficits in specification of sympathetic neuronal types in $Nt3^{-/-}$ mice, TH and DBH expression has been examined prior to normal cell death (i.e., at E15). TH and DBH in the superior cervical ganglion of $Nt3^{-/-}$ and $TrkA^{-/-}$ mice but not $Ngf^{-/-}$ mice display deficits of expression, suggesting that NT3 can act via TRKA to regulate their expression (Andres *et al*, 2008). Thus, much of the previously known functions of NT3 during sympathetic neuron development may include interactions and signalling via TRKA in the $TRKA^{+}$ noradrenergic lineage. Alternative splicing generates transcripts that encode both TRKC receptors with and without the catalytic tyrosine kinase domain.

Quantitative PCR data show that transcripts lacking the tyrosine kinase domain are expressed at much greater levels than transcripts encoding catalytic full-length TRKC receptors in developing sympathetic neurons (Wyatt *et al*, 1997), supporting a ligand-independent activity of TRKC during sympathetic neuron diversification. In contrast to this conclusion, NT3 has been shown to induce *ChAT* and *Vip* expression in cultured E12 sympathetic neurons in a mechanism likely not involving TRKA since unlike NT3, NGF fails to induce ChAT and VIP (Brodski *et al*, 2000, 2002). This indicates that sympathetic precursors express sufficient amounts of catalytically active TRKC receptors for a functional response. It is therefore unclear whether the role of TRKC for sympathetic diversification in the present study is ligand dependent or ligand independent. If it does involve a ligand interaction, then $Nt3^{-/-}$ mice are expected to display a much more complex phenotype than $TrkC^{-/-}$ mice as NT3 may also interact with other receptors, such as TRKA during sympathetic neuron development.

The roles of TRKC during cholinergic sympathetic neuron differentiation described in the present study may partly involve its repressive activity on *Hmx1* expression in sympathetic precursors, because HMX1 represses *Ret*, and hence suppression of *Hmx1* expression by TRKC activity is compatible with continuous expression of *Ret*. Mice with null mutations in *Ret*, or one of its ligand, artemin or the artemin co-receptor GFRα3 display short and misdirected proximal axon projections (Schuchardt *et al*, 1994; Nishino *et al*, 1999; Enomoto *et al*, 2001; Honma *et al*, 2002), suggesting that both RET and TRKC work in the sympathetic precursors to induce extension of proximal axons. As precursors diversify into defined neurotransmitter classes of sympathetic neurons RET is absolutely critical for defining the cholinergic phenotype as seen by the failure of *Chat*, *VAChT*, *Sst* and *Vip* expression in *Ret* mutant mice. These results are consistent with previous data which has established that an RET ligand, GDNF, induces ChAT *in vitro* (Brodski *et al*, 2002), and that loss of RET in mutant mice markedly reduces the number of $ChAT^+$ and $VAChT^+$ neurons at E16 (Burau *et al*, 2004). We found that the loss of cholinergic sympathetic neurons in $Ret^{CFP/CFP}$ mice was paralleled by an increase in noradrenergic $HMX1^+$ and $TRKA^+$ neurons, which represents a true switch in fate, because cholinergic neurons that normally should have expressed *Ret*, acquired *Hmx1* expression as determined in $Ret^{CFP/CFP}$;$Hmx1^{LcZ/+}$ mice. Hence, RET induces a cholinergic fate also by aborting expression of key factors necessary for noradrenergic fate. We identified HMX1 as one such factor, since $HMX1^+$ neurons were markedly elevated in $Ret^{CFP/CFP}$;$Hmx1^{LcZ/+}$ mice. Consistently, $TRKA^+$ neurons were increased proportionally to the increase in $HMX1^+$ cells.

Tlx3 was found to be expressed in most or all sympathetic precursors but was rapidly downregulated in cells attaining *Hmx1* expression and was later in development confined only to the cholinergic sympathetic lineage. In the sympathetic lineage, we observe that *Tlx3* and *Ret* are always co-expressed, first in most or all precursors and later in the diversifying cholinergic lineage. The diversification of HMX1 and TLX3 along different sympathetic lineages can be explained by the suppressive activities of HMX1 on *Tlx3*, as observed by a continuous expression of *Tlx3* in most neurons of $Hmx1^{fl/fl}$;*Wnt1-Cre* mice. RET can act as a positive regulator of *Tlx3* expression in cultures of the chick sympathetic chain (Apostolova *et al*, 2007). Hence, a failure of RET repression in $Hmx1^{fl/fl}$;*Wnt1-Cre* mice might mediate the sustained *Tlx3* expression. Thus, cholinergic neurons develop in a process involving sustained TRKC activity in sympathetic precursors, preventing *Hmx1* induction and therefore persistent *Tlx3*/*Ret* expression that consolidates a cholinergic fate by RET-dependent induction and maintenance of cholinergic neuronal properties and a sustained repression of *Hmx1*.

In conclusion, our data support a model in which a hybrid noradrenergic/cholinergic sympathetic precursor diversifies in a highly controlled hierarchical segregation into distinct sympathetic types. This segregation of a common precursor into distinct neuronal types involves an intricate process based on repressive cross-regulatory interactions comprising both transcriptional activities and growth factor receptor activities, which defines the fate and function of the neurons.

Materials and methods

Generation of Hmx1 conditional null mice

Figure 3A and supporting information Supplementary Figure S5A and G show the targeting strategy used to generate mice carrying a conditional knockout allele of *Hmx1* (Taconic-Artemis, Germany). The targeting vector with a 5.8-kb long arm and 3.0-kb short arm (Figure 3A; Supplementary Figure S5) was generated using BAC clones from the C57BL/6J RPCI-23 BAC library. The 5′ LoxP DNA sequence, the target for the Cre recombinase, was inserted in the first intron. The second LoxP site was placed 3′ to the second exon. The positive selection marker NeoR, which confers G418 (neomycin) resistance, was flanked by FRT sites that can be cleaved by the Flp-Deleter Flipase recombinase (Flpe); the negative selection marker Thymidine kinase (Tk) cassette, which confers Gancyclovir resistance, was placed 5′ to the long arm of homology. The linearized targeting vector was transfected into ES cells (Supplementary Figure S5A–E). Homologous recombinant clones were isolated using positive (neomycin) and negative (gancyclovir) selection. Hybridization of Southern blots was used on genomic DNA to detect homologous recombination and single integration at the 5′ side was performed using *Eco*RI, *Bcl*I and *Pfl*FI restriction enzymes and ila2 probe, which gave 13.6, 13.7 and 11.6 kb fragments, respectively, for the wild-type allele and a 7.8-, 11.9- and 8.4-kb fragment for the targeted allele (not shown). Southern hybridization on the 3′ side was performed by digestion with *Eco*RI, *Afl*II, *Hin*dIII and 3e1 probe produced 13.6, 17.9 and 8.1 kb fragments, respectively, for the wild-type allele and a 5.4-, 5.2-, 9.2-kb fragment for the targeted allele (not shown). ES clones were injected into 3.5 days post coitum (dpc) blastocysts derived from super-ovulated BALB/c females mated with BALB/c males. Injected blastocysts were the transferred to each uterine horn of 2.5 dpc, pseudopregnant NMRI females. Chimeric mice were bred to strain BALB/c females in order to generate heterozygous mice carrying the targeted allele. These mice were bred with a Flp-Deleter mouse line, removing the neo cassette and creating mice carrying the *Hmx1* floxed allele, referred to as $Hmx1^{fl}$. $Hmx1^{fl}$ mice were then bred with *Wnt1-Cre* mice to remove the second exon (containing the homeobox domain) and generating a conditional knock-out mouse ($Hmx1^{fl/fl}$;*Wnt1-Cre*). Genotyping for mice carrying the *Hmx1* floxed allele and Wnt1-Cre was performed by PCR (Supplementary Figure S5F). The following primers were used: 5′-CCTGGTGACATCCCTTGTACG-3′ and 5′-GGGTGACATTGGCACAACC-3′, to detect both the wild-type allele (218-bp band) and the floxed allele (375-bp band) of *Hmx1* (Supplementary Figure S5G) and 5′-ACCAGGTTCGTTCACTCATGG-3′ (Forward) and 5′-AGGCTAAGTGC CTTCTCTACA-3′ (Reverse) to detect the *Wnt1-Cre* allele (200 bp). Successful elimination of *Hmx1* in the SG was confirmed by *in situ* hybridization (Supplementary Figure S5H).

The $Hmx1^{LcZ}$ ES line was purchased from Velocigene, injected into 3.5 dpc blastocyst to generate chimeric mice that were bred for germline transmission and used as heterozygous mice for detection of *Hmx1* expression (for further details, refer to Supplementary Figure S2A–C).

Other mice strains

Bax$^{-/-}$, *TrkC*$^{-/-}$, *Wnt1-Cre* and *Gt(ROSA)26*$^{tm9(CAG\text{-}tdTomato)}$ mice were ordered from The Jackson Laboratory. Genotyping of the *Gt(ROSA)26*$^{tm9(CAG\text{-}tdTomato)}$ mice was performed by PCR. The following primers: 5′-AAAGTCGCTCTGAGTTGTTAT-3′ (Forward wild-type) and 5′-GGAGCGGGAGAAATGGATATG-3′ (Reverse wild-type) and 5′-TGGCGTTACTATGGGAACAT-3′ (Reverse Tomato) were used to detect both the wild-type allele (500 bp band) and the tomato allele (407 bp band). *Ret*^{CFP} and *Ret*^{ERT2} mice have been described previously (Uesaka *et al*, 2008; Luo *et al*, 2009).

Immunohistochemistry

Embryos were collected and fixed in 4% paraformaldehyde (PFA) in PBS (pH 7.4) at 4°C for 1–3 h. The lower thoracic sympathetic chain (vertebrae 9th to 13th) was dissected out together with the spinal cord and fixed in 4% PFA in PBS for 5 h. Samples were subsequently washed in PBS at 4°C for 1 h and cryoprotected by incubating at 4°C overnight in 20% sucrose followed by 30% sucrose in PBS. Tissues were then embedded in OCT and frozen at −20°C. Samples were sectioned at 14 μm and frozen at −20°C after drying at RT for 1 h. In order to have a complete representation of the 9th to 13th thoracic paravertebral SG, sections were serially collected on 10–12 slides. For every condition, each slide contained tissues from two embryos or pups, belonging to the same litter.

For immunohistochemistry, fresh frozen sections were used and dried at RT for 1 h. For RET and ISL1 staining, particularly at postnatal stages, antigen retrieval was performed by immersing the sections in 80°C antigen retrieval solution (DAKO) for 20 min. Sections were then washed three times in PBS containing 0.1% Tween-20 (PBSt), incubated with primary antibodies diluted in PBSt at 4°C overnight and coverslipped with parafilm. Sections were then washed in PBSt and incubated with secondary antibodies diluted in PBSt at room temperature for 1 h, washed again in PBSt and mounted using glycerol. For detection of Ret^{CFP}, anti-GFP (FITC) antibody (Abcam) was diluted at 1:500 and incubated for 2 h following secondary antibody staining. The primary antibodies used were Goat anti-VAChT (Phoenix Europe GmbH, 1:400 dilution), Rabbit anti-VMAT2 (Phoenix Europe GmbH, 1:150), Sheep anti-TH (Novus Biologicals, 1:2000), Rabbit anti-TH (Pel-Freez, 1:1000), Goat anti-TRKC (R&D, 1:500), Goat anti-ChAT (Millipore, 1:100), Rabbit anti-DBH (Protos Immunoresearch, 1:100), Rabbit anti-PRPH (Chemicon International, 1:500), Goat anti-RET (R&D, 1:50), Sheep anti-NPY (Abcam 1:1000), Goat anti-TRKA (R&D, 1:500), Rabbit anti-TRKA (kind gift from Louis Reichardt), Rabbit anti-TRKA (Millipore, 1:1000), Goat anti-TRKC (R&D, 1:500), Goat anti-CGRP (Abcam, 1:1000), Rabbit anti-VIP (Immunostar, 1:200), Rat anti-SST (Millipore, 1:100), Chicken anti-βgal (Abcam, 1:1500), Rabbit anti-Phox2A/B (kind gift from Jean-François Brunet, 1:400), Rabbit and Guinea Pig anti-TLX3 (kind gift from Thomas Müller and Carmen Birchmeier, 1:10 000), Mouse anti-ISL1 (Developmental Studies Hybridoma Bank (DSHB), 1:100), ASMA-Cy3 (Sigma-Aldrich, 1:100), Rabbit anti-PGP9.5 (AbD Serotec, 1:1000). The secondary antibodies used were Alexa 555 or 647 conjugated donkey anti-mouse antibody, Alexa 488, 555 or 647 conjugated donkey anti-rabbit, Alexa 488, 555 or 647 conjugated donkey anti-goat, Alexa 488 or 555 conjugated donkey anti-sheep, Alexa 488 or 555 conjugated goat anti-rat, Alexa 549-donkey anti-chicken, Alexa 488 or 555 conjugated donkey anti-sheep. All secondary antibodies were purchased from Invitrogen and used at 1:1000 dilution.

In situ hybridization

Tissue was processed as for immunohistochemistry, and hybridizations were performed as previously described (Adameyko *et al*, 2009). pCRII-*Hmx1* cDNA plasmid (kind gift from Thomas Lufkin, Genome Institute of Singapore) was used to synthesize digoxigenin antisense riboprobes according to supplier's instructions (Roche, Mannheim, Germany). Visualization was carried out using alkaline phosphatase-conjugated anti-digoxigenin antibodies (Roche, 1:2000) followed by alkaline phosphatase staining developed with NBT/BCIP (Roche).

Tamoxifen injections

Tamoxifen (4-HT, Sigma) was dissolved in corn oil (Sigma). Tamoxifen solution was delivered via intra-peritoneal (i.p.) injection to pregnant females at E11.5 and 3-day-old pups (100 μg/g of 4-HT body weight). For all experiments, the day of the plug positive was considered as E0.5 and P0 the day when the mice were born.

Quantification and statistics

Hmx1 (recapitulated by βgal), *TrkA*, *Ret*, *Vmat2*, *VAChT*, *Phox2a/b*, *TrkC*, *Sst*, *Prph2* and *Npy* expression was analysed in SG sections from *Hmx1*$^{LcZ/+}$ (E12.5, E13.5, E14.5 and E15.5) or *RET*$^{CFP/+}$;*Hmx1*$^{LcZ/+}$ (E18.5, P5 and P11) animals. In the latter case, *Ret*^{CFP} was detected using FITC-conjugated anti-GFP antibody. For quantification, at least six SG sections from at least two animals were counted for every developmental stage. For quantification of the RET$^+$, TRKA$^+$, TH$^+$, PHOX2A/B$^+$, SST$^+$, VIP$^+$, NPY$^+$, ChAT$^+$, VAChT$^+$, DBH$^+$, VMAT2$^+$, CGRP$^+$ and TLX3$^+$ populations in control and *Hmx1* mutants, at least six SGs from at least three animals for each genotype and stage were analysed. For *Ret*$^{-/-}$ analysis, quantification of TRKC$^+$, SST$^+$, VIP$^+$ and VAChT$^+$ neurons was carried on control (*RET*$^{CFP/+}$) and mutant *Ret* (*Ret*$^{CFP/CFP}$) E15.5 embryos; quantification of *Hmx1* and *TrkA* expression was carried out in control (*Ret*$^{CFP/+}$;*Hmx1*$^{LcZ/+}$) and mutant *Ret* (*Ret*$^{CFP/CFP}$;*Hmx1*$^{LcZ/+}$) E14.4 and E15.5 embryos. In both cases, at least eight SG sections from at least two embryos were counted. For quantification of (mRNA)*Hmx1*$^+$, TRKA$^+$, RET$^+$, TH$^+$ and ChAT$^+$ neurons in control and *TrkC*$^{-/-}$ and *TrkC*$^{-/-}$;*Bax*$^{-/-}$ mutants at E15.5, E18.5 and P0 at least 15 randomly selected SG per animal per stage were counted. For all counts, the number of positive neurons was normalized to the total number of ISL1$^+$ neurons in each ganglion. For quantification of the number of paravertebral sympathetic neurons in wild-type and *Hmx1*$^{fl/fl}$;*Wnt1-Cre* mice, 14–43 SG from three newborn (P0) pups were analysed. Data were analysed using GraphPad Prism 5 and expressed as mean ± standard error of mean (s.e.m.). Unpaired Student's *t*-test was performed to determine if there were significant differences between groups.

Supplementary data

Supplementary data are available at *The EMBO Journal* Online (http://www.embojournal.org).

Acknowledgements

We thank Jean-François Brunet, Louis Reichardt and Thomas Müller and Carmen Birchmeier, for generously providing Phox2a/b, TrkA and Tlx3 antibody, respectively. We also thank Helena Samuelsson for her technical support. This work was supported by the Swedish Medical Research Council, Knut and Alice Wallenbergs Foundation (Wallenberg Scholar and for CLICK imaging facility), Linné grants (DBRM grants), Swedish Cancer Foundation, the Swedish Brain Foundation, Hållsten Foundation, EU FP7 MOLPARK collaborative project, Söderbergs Foundation and ERC advanced grant (232675) and Karolinska Institutet.

Author contributions: AF, FL and PE designed the study. FL and PE supervised the study. AF performed most of the experiments, analysed the data and prepared the Figures. ML and IA performed some experiments. AF and PE wrote the paper, with input from all co-authors.

Conflict of interest

The authors declare that they have no conflict of interest.

References

Adameyko I, Lallemend F, Aquino JB, Pereira JA, Topilko P, Muller T, Fritz N, Beljajeva A, Mochii M, Liste I, Usoskin D, Suter U, Birchmeier C, Ernfors P (2009) Schwann cell precursors from nerve innervation are a cellular origin of melanocytes in skin. *Cell* **139:** 366–379

Anderson CR, Bergner A, Murphy SM (2006) How many types of cholinergic sympathetic neuron are there in the rat stellate ganglion? *Neuroscience* **140:** 567–576

Andres R, Herraez-Baranda LA, Thompson J, Wyatt S, Davies AM (2008) Regulation of sympathetic neuron differentiation by endogenous nerve growth factor and neurotrophin-3. *Neurosci Lett* **431:** 241–246

Apostolova G, Dechant G (2009) Development of neurotransmitter phenotypes in sympathetic neurons. *Auton Neurosci* **151:** 30–38

Apostolova G, Dorn R, Ka S, Hallbook F, Lundeberg J, Liser K, Hakim V, Brodski C, Michaelidis TM, Dechant G (2007) Neurotransmitter phenotype-specific expression changes in developing sympathetic neurons. *Mol Cell Neurosci* **35:** 397–408

Asmus SE, Parsons S, Landis SC (2000) Developmental changes in the transmitter properties of sympathetic neurons that innervate the periosteum. *J Neurosci* **20:** 1495–1504

Asmus SE, Tian H, Landis SC (2001) Induction of cholinergic function in cultured sympathetic neurons by periosteal cells: cellular mechanisms. *Dev Biol* **235:** 1–11

Brennan C, Rivas-Plata K, Landis SC (1999) The p75 neurotrophin receptor influences NT-3 responsiveness of sympathetic neurons in vivo. *Nat Neurosci* **2:** 699–705

Brodski C, Schaubmar A, Dechant G (2002) Opposing functions of GDNF and NGF in the development of cholinergic and noradrenergic sympathetic neurons. *Mol Cell Neurosci* **19:** 528–538

Brodski C, Schnurch H, Dechant G (2000) Neurotrophin-3 promotes the cholinergic differentiation of sympathetic neurons. *Proc Natl Acad Sci USA* **97:** 9683–9688

Burau K, Stenull I, Huber K, Misawa H, Berse B, Unsicker K, Ernsberger U (2004) c-ret regulates cholinergic properties in mouse sympathetic neurons: evidence from mutant mice. *Eur J Neurosci* **20:** 353–362

Crowley C, Spencer SD, Nishimura MC, Chen KS, Pitts-Meek S, Armanini MP, Ling LH, McMahon SB, Shelton DL, Levinson AD, Phillips HS (1994) Mice lacking nerve growth factor display perinatal loss of sensory and sympathetic neurons yet develop basal forebrain cholinergic neurons. *Cell* **76:** 1001–1011

Davies AM, Minichiello L, Klein R (1995) Developmental changes in NT3 signalling via TrkA and TrkB in embryonic neurons. *EMBO J* **14:** 4482–4489

ElShamy WM, Linnarsson S, Lee KF, Jaenisch R, Ernfors P (1996) Prenatal and postnatal requirements of NT-3 for sympathetic neuroblast survival and innervation of specific targets. *Development* **122:** 491–500

Enomoto H, Crawford PA, Gorodinsky A, Heuckeroth RO, Johnson Jr EM, Milbrandt J (2001) RET signaling is essential for migration, axonal growth and axon guidance of developing sympathetic neurons. *Development* **128:** 3963–3974

Ernfors P, Merlio JP, Persson H (1992) Cells expressing mRNA for neurotrophins and their receptors during embryonic rat development. *Eur J Neurosci* **4:** 1140–1158

Ernsberger U, Rohrer H (1999) Development of the cholinergic neurotransmitter phenotype in postganglionic sympathetic neurons. *Cell Tissue Res* **297:** 339–361

Fagan AM, Zhang H, Landis S, Smeyne RJ, Silos-Santiago I, Barbacid M (1996a) TrkA, but not TrkC, receptors are essential for survival of sympathetic neurons in vivo. *J Neurosci* **16:** 6208–6218

Fagan AM, Zhang H, Landis S, Smeyne RJ, Silos-Santiago I, Barbacid M (1996b) TrkA, but not TrkC, receptors are essential for survival of sympathetic neurons in vivo. *J Neurosci* **16:** 6208–6218

Francis N, Farinas I, Brennan C, Rivas-Plata K, Backus C, Reichardt L, Landis S (1999) NT-3, like NGF, is required for survival of sympathetic neurons, but not their precursors. *Dev Biol* **210:** 411–427

Francis NJ, Landis SC (1999) Cellular and molecular determinants of sympathetic neuron development. *Annu Rev Neurosci* **22:** 541–566

Ghasemlou N, Krol KM, Macdonald DR, Kawaja MD (2004) Comparison of target innervation by sympathetic axons in adult wild type and heterozygous mice for nerve growth factor or its receptor trkA. *J Pineal Res* **37:** 230–240

Glebova NO, Ginty DD (2004) Heterogeneous requirement of NGF for sympathetic target innervation in vivo. *J Neurosci* **24:** 743–751

Glebova NO, Ginty DD (2005) Growth and survival signals controlling sympathetic nervous system development. *Annu Rev Neurosci* **28:** 191–222

Goridis C, Rohrer H (2002) Specification of catecholaminergic and serotonergic neurons. *Nat Rev Neurosci* **3:** 531–541

Guillemot F, Lo LC, Johnson JE, Auerbach A, Anderson DJ, Joyner AL (1993) Mammalian achaete-scute homolog 1 is required for the early development of olfactory and autonomic neurons. *Cell* **75:** 463–476

Habecker BA, Landis SC (1994) Noradrenergic regulation of cholinergic differentiation. *Science* **264:** 1602–1604

Hirsch MR, Tiveron MC, Guillemot F, Brunet JF, Goridis C (1998) Control of noradrenergic differentiation and Phox2a expression by MASH1 in the central and peripheral nervous system. *Development* **125:** 599–608

Honma Y, Araki T, Gianino S, Bruce A, Heuckeroth R, Johnson E, Milbrandt J (2002) Artemin is a vascular-derived neurotropic factor for developing sympathetic neurons. *Neuron* **35:** 267–282

Howard MJ (2005) Mechanisms and perspectives on differentiation of autonomic neurons. *Dev Biol* **277:** 271–286

Kuruvilla R, Zweifel LS, Glebova NO, Lonze BE, Valdez G, Ye H, Ginty DD (2004) A neurotrophin signaling cascade coordinates sympathetic neuron development through differential control of TrkA trafficking and retrograde signaling. *Cell* **118:** 243–255

Levi-Montalcini R (1987) The nerve growth factor 35 years later. *Science* **237:** 1154–1162

Lo L, Morin X, Brunet JF, Anderson DJ (1999) Specification of neurotransmitter identity by Phox2 proteins in neural crest stem cells. *Neuron* **22:** 693–705

Lo L, Tiveron MC, Anderson DJ (1998) MASH1 activates expression of the paired homeodomain transcription factor Phox2a, and couples pan-neuronal and subtype-specific components of autonomic neuronal identity. *Development* **125:** 609–620

Lucas ME, Muller F, Rudiger R, Henion PD, Rohrer H (2006) The bHLH transcription factor hand2 is essential for noradrenergic differentiation of sympathetic neurons. *Development* **133:** 4015–4024

Luo W, Enomoto H, Rice FL, Milbrandt J, Ginty DD (2009) Molecular identification of rapidly adapting mechanoreceptors and their developmental dependence on ret signaling. *Neuron* **64:** 841–856

Morikawa Y, D'Autreaux F, Gershon MD, Cserjesi P (2007) Hand2 determines the noradrenergic phenotype in the mouse sympathetic nervous system. *Dev Biol* **307:** 114–126

Morin X, Cremer H, Hirsch MR, Kapur RP, Goridis C, Brunet JF (1997) Defects in sensory and autonomic ganglia and absence of locus coeruleus in mice deficient for the homeobox gene Phox2a. *Neuron* **18:** 411–423

Morris JL, Grasby DJ, Anderson RL, Gibbins IL (1998) Neurochemical distinction between skeletal muscle vasodilator neurons and pelvic vasodilator neurons in guinea-pigs. *J Auton Nerv Syst* **71:** 64–68

Munroe RJ, Prabhu V, Acland GM, Johnson KR, Harris BS, O'Brien TP, Welsh IC, Noden DM, Schimenti JC (2009) Mouse H6 Homeobox 1 (Hmx1) mutations cause cranial abnormalities and reduced body mass. *BMC Dev Biol* **9:** 27

Nishino J, Mochida K, Ohfuji Y, Shimazaki T, Meno C, Ohishi S, Matsuda Y, Fujii H, Saijoh Y, Hamada H (1999) GFR alpha3, a component of the artemin receptor, is required for migration and survival of the superior cervical ganglion. *Neuron* **23:** 725–736

Otten U, Katanaka H, Thoenen H (1978) Role of cyclic nucleotides in NGF-mediated induction of tyrosine hydroxylase in rat sympathetic ganglia and adrenal medulla. *Brain Res* **140:** 385–389

Patel TD, Jackman A, Rice FL, Kucera J, Snider WD (2000) Development of sensory neurons in the absence of NGF/TrkA signaling in vivo. *Neuron* **25:** 345–357

Pattyn A, Morin X, Cremer H, Goridis C, Brunet JF (1997) Expression and interactions of the two closely related homeobox genes Phox2a and Phox2b during neurogenesis. *Development* **124:** 4065–4075

Pattyn A, Morin X, Cremer H, Goridis C, Brunet JF (1999) The homeobox gene Phox2b is essential for the development of autonomic neural crest derivatives. *Nature* **399:** 366–370

Schneider C, Wicht H, Enderich J, Wegner M, Rohrer H (1999) Bone morphogenetic proteins are required in vivo for the generation of sympathetic neurons. *Neuron* **24:** 861–870

Schorderet DF, Nichini O, Boisset G, Polok B, Tiab L, Mayeur H, Raji B, de la Houssaye G, Abitbol MM, Munier FL (2008) Mutation in the human homeobox gene NKX5-3 causes an oculo-auricular syndrome. *Am J Hum Genet* **82:** 1178–1184

Schotzinger R, Yin X, Landis S (1994) Target determination of neurotransmitter phenotype in sympathetic neurons. *J Neurobiol* **25:** 620–639

Schuchardt A, D'Agati V, Larsson-Blomberg L, Costantini F, Pachnis V (1994) Defects in the kidney and enteric nervous system of mice lacking the tyrosine kinase receptor Ret. *Nature* **367:** 380–383

Smeyne RJ, Klein R, Schnapp A, Long LK, Bryant S, Lewin A, Lira SA, Barbacid M (1994) Severe sensory and sympathetic neuropathies in mice carrying a disrupted Trk/NGF receptor gene. *Nature* **368:** 246–249

Stanke M, Junghans D, Geissen M, Goridis C, Ernsberger U, Rohrer H (1999) The Phox2 homeodomain proteins are sufficient to promote the development of sympathetic neurons. *Development* **126:** 4087–4094

Tessarollo L, Tsoulfas P, Donovan MJ, Palko ME, Blair-Flynn J, Hempstead BL, Parada LF (1997) Targeted deletion of all isoforms of the trkC gene suggests the use of alternate receptors by its ligand neurotrophin-3 in neuronal development and implicates trkC in normal cardiogenesis. *Proc Natl Acad Sci USA* **94:** 14776–14781

Uesaka T, Nagashimada M, Yonemura S, Enomoto H (2008) Diminished Ret expression compromises neuronal survival in the colon and causes intestinal aganglionosis in mice. *J Clin Investig* **118:** 1890–1898

Wyatt S, Pinon LG, Ernfors P, Davies AM (1997) Sympathetic neuron survival and TrkA expression in NT3-deficient mouse embryos. *EMBO J* **16:** 3115–3123

Xu H, Firulli AB, Zhang X, Howard MJ (2003) HAND2 synergistically enhances transcription of dopamine-beta-hydroxylase in the presence of Phox2a. *Dev Biol* **262:** 183–193

Yoshiura K, Leysens NJ, Reiter RS, Murray JC (1998) Cloning, characterization, and mapping of the mouse homeobox gene Hmx1. *Genomics* **50:** 61–68

Zhang D, Mehler MF, Song Q, Kessler JA (1998) Development of bone morphogenetic protein receptors in the nervous system and possible roles in regulating trkC expression. *J Neurosci* **18:** 3314–3326